

See discussions, stats, and author profiles for this publication at: <https://www.researchgate.net/publication/231235601>

# Synthesis of Hydrophobic Molecular Sieves by Hydrothermal Treatment with Acetic Acid

ARTICLE *in* CHEMISTRY OF MATERIALS · JANUARY 2001

Impact Factor: 8.35 · DOI: 10.1021/cm0007961

---

CITATIONS

32

---

READS

12

4 AUTHORS, INCLUDING:



Mark Davis

California Institute of Technology

497 PUBLICATIONS 30,653 CITATIONS

SEE PROFILE

# Synthesis of Hydrophobic Molecular Sieves by Hydrothermal Treatment with Acetic Acid

Christopher W. Jones,<sup>\*,†,‡</sup> Son-Jong Hwang,<sup>†</sup> Tatsuya Okubo,<sup>§</sup> and Mark E. Davis<sup>†</sup>

*Division of Chemistry and Chemical Engineering, California Institute of Technology, Pasadena, California 91125, and Department of Chemical System Engineering, University of Tokyo, Bunkyo-ku, Tokyo, 113-8656, Japan*

*Received October 4, 2000. Revised Manuscript Received December 9, 2000*

A series of calcined borosilicate molecular sieves are treated hydrothermally with aqueous acetic acid and subsequently characterized in detail. The acid treatments are shown to expel boron from the molecular sieves, and the defects created by the boron removal are subsequently healed with silicon dissolved from other parts of the crystal. By use of this procedure, highly crystalline, hydrophobic all-silica CIT-1 and SSZ-33 (CON topology) molecular sieves are synthesized for the first time. <sup>29</sup>Si Bloch decay (BD) and cross-polarization magic-angle spinning (CPMAS) NMR spectra indicate that the materials have few internal defects and allow for structural characterization of CON materials by <sup>29</sup>Si MAS NMR. Seven unique tetrahedral silicon species are identified in the spectra in agreement with the published crystal structure. The effects of treatment conditions such as acid type, solution pH, and temperature are studied in detail. Conditions near the isoelectric point of silica (pH = 0–2) are found to be efficient for the production of a variety of hydrophobic materials with few structural defects including molecular sieves of the \*BEA, CON, and MWW topologies. Detailed control studies using SSZ-33 show that the nearly defect-free materials contain triangular mesopores that are clearly distinguishable in field-emission electron microscopy images. The silica that previously inhabited the mesopores is a likely source for the species required to heal the defects created by boron expulsion. In addition to healing the vacancies previously inhabited by boron with dissolved silicon, an additional aluminum or gallium source can be added to the acetic acid solution and the ions are incorporated into the framework. Many of the defects that are not filled with the Al<sup>3+</sup> or Ga<sup>3+</sup> species are filled with silicon during the treatment to produce a more hydrophobic metallosilicate than the one containing internal silanol defects.

## Introduction

Hydrophobic, pure-silica zeolites are useful materials primarily because of their organophilic character and thermal and hydrothermal stability. Microporous, pure-silica molecular sieves can be synthesized hydrothermally using organic molecules, structure-directing agents (SDAs), to kinetically steer their syntheses to the desired products. However, in many cases, the presence (or absence) of tetrahedral, non-silicon atoms in the synthesis such as boron, aluminum, or zinc causes the formation of different crystalline phases or prevents the formation of a crystalline phase entirely. For example, the use of the *N,N,N*-trimethyl-2-adamantanammonium cation as an SDA gives SSZ-24 (AFI) when boron is included in the synthesis gel, and SSZ-13, SSZ-23, or SSZ-25 when varying amounts of aluminum are included in the synthesis.<sup>1</sup> In the absence of any tetra-

hedral, non-silicon atom in the synthesis, no crystalline products are formed. Situations such as this invariably arise in zeolite synthesis and as a result, many framework topologies can only be synthesized in a narrow range of framework compositions. For example, molecular sieves of the CON topology have only been directly synthesized to date as borosilicates (SSZ-33,<sup>2</sup> CIT-1)<sup>3</sup> or as an aluminosilicate (SSZ-26).<sup>4</sup>

To access other framework compositions, various strategies have been employed. Dealumination of zeolites is commonly carried out to synthesize high-silica or pure-silica zeolites. Many dealumination procedures have been developed over the years including steaming,<sup>5</sup> treatment with mineral acids<sup>6</sup> or chelating agents,<sup>7</sup> reaction with silicon tetrachloride<sup>8</sup> and treatment with silicon hexafluoride.<sup>9</sup>

\* E-mail: chris.jones@che.gatech.edu.

† California Institute of Technology.

‡ Current address: School of Chemical Engineering, Georgia Institute of Technology, Atlanta, GA 30332.

§ University of Tokyo.

(1) Zones et al. In *Proceedings of the 9th International Zeolite Conference*; von Ballmoos, R., et al., Eds.; Butterworth-Heinemann: Boston, MA, 1993; p 163.

(2) Zones, S. I. U.S. Patent 4,963,337, 1990.

(3) Lobo, R. F.; Davis, M. E. *J. Am. Chem. Soc.* **1995**, *117*, 3764.

(4) Zones, S. I.; Olmstead, M. M.; Santilli, D. S. *J. Am. Chem. Soc.* **1992**, *114*, 4195.

(5) McDaniel, C. V.; Maher, P. K. In *Molecular Sieves*; Barrer, R. M., Ed.; Society of Chemical Industry: London, 1968; p 186; U.S. Patent 3,449,070, 1969.

(6) Barrer, R. M.; Makki, M. B. *Can. J. Chem.* **1964**, *42*, 1481.

(7) Kerr, G. T. *J. Phys. Chem.* **1968**, *72*, 2594.

(8) Beyer, H. K.; Belenkykaja, I. In *Catalysis by Zeolites*; Imelik, B., et al., Eds.; Elsevier: Amsterdam, 1980; p 203.

Another route to both all-silica and heteroatom-containing framework compositions is through the use of borosilicates as precursor species. Removal of boron from the framework of molecular sieves requires significantly milder conditions than does the removal of aluminum.<sup>10</sup> Vacancies with tetrahedral coordination can then be repopulated in a subsequent step with a variety of species including silicon,<sup>10</sup> titanium,<sup>11</sup> and aluminum,<sup>2</sup> among others.

Recently, the zincosilicate CIT-6 (\*BEA topology) was synthesized and extensively characterized.<sup>12–13</sup> This material is unique because it can be used as a precursor to a variety of molecular sieves of the \*BEA structure. The organic SDA can be removed from the micropores by solvent extraction techniques. Furthermore, zinc, like boron, can easily be removed from the molecular sieve framework under relatively mild conditions. In particular, aqueous acetic acid treatments were found to be suitable for removal of zinc from the framework of CIT-6 while simultaneously removing the organic SDA from the micropores. Under the proper conditions, zinc can completely be removed from the material, and the vacancies (defects) left behind can be healed with silicon that is presumably dissolved from other parts of the crystal. Similarly, in the development of organic-functionalized molecular sieves (OFMSs), we found that extraction of the organic SDA from the micropores of the molecular sieve using aqueous acetic acid resulted in materials that were essentially free of structural defects.<sup>14</sup> In contrast, extraction with other solvents left a material that contained a significant number of internal defects as determined by <sup>29</sup>Si solid-state NMR spectroscopy.

In this work, we report the extension of the use of acetic acid treatment to a variety of calcined molecular sieves with different framework compositions and structures and show the generality of this methodology for preparing a broad spectrum of molecular sieve materials. Here, calcined borosilicate and pure-silica molecular sieves of different topologies are treated with acetic acid under a variety of conditions and are subsequently characterized in detail. Specific attention is paid to the role of acetic acid in this system.

## Experimental Section

**Molecular Sieve Synthesis.** Borosilicate CIT-1 (CON topology) was synthesized via the published procedure using *N,N,N*-trimethyl (+)myrtanlylammonium hydroxide as an SDA in a Teflon-lined autoclave at 160 °C.<sup>3</sup> Borosilicate SSZ-33 (CON topology) was synthesized as described in the literature.<sup>2</sup> The borosilicate of the MWW topology, ERB-1, was prepared using a published procedure.<sup>15</sup> Aluminum-free, boron-containing ZSM-5 (MFI topology) was synthesized using the procedure

reported by Dwyer.<sup>16</sup> Silicalite, the all-silica variant of ZSM-5, was synthesized in the absence of alkali metal ions using a mixture of tetrapropylammonium bromide and piperazine as SDAs. Molecular sieves with the BEA topology were synthesized in a variety of forms. Borosilicate<sup>14</sup> and pure-silica<sup>14,17</sup> Beta molecular sieves were synthesized using tetraethylammonium fluoride as the SDA. These samples are denoted as B-Beta-F and Si-Beta-F, respectively. Pure-silica Beta was also synthesized using 4,4'-trimethylenebis(1-methyl-1-benzylpiperidinium) hydroxide as an SDA using a published procedure.<sup>18</sup> This material is denoted as Si-Beta-OH. A borosilicate Beta sample, referred to as B-Beta-OH, was also synthesized in hydroxide media following an established method.<sup>19</sup> All materials were calcined to remove the occluded structure-directing agent. Samples were heated in an oven at approximately 2 °C/min in a nitrogen purge up to the maximum temperature of 500–675 °C at which point air was fed to the oven for 4–8 h.

**Acetic Acid Treatment.** For experiments at temperatures above 100 °C, calcined molecular sieves were treated in Teflon-lined autoclaves in an oven with rotation at ~60 rpm for 6 days unless noted. In a typical experiment, 0.2 g of molecular sieve was added to a 45 mL autoclave filled with 25 g of water and 10 g of glacial acetic acid (pH ~ 1.65). After 144 h of heating, the autoclave was cooled rapidly in a water bath, and the solid products were washed extensively with water and acetone and recovered by filtration. Any variations on this scheme are noted specifically in the text.

**Analysis.** X-ray powder diffraction (XRD) patterns were collected on a Scintag XDS 2000 diffractometer using Cu-K $\alpha$  radiation. <sup>11</sup>B, <sup>27</sup>Al, and <sup>29</sup>Si NMR spectra were recorded on a Bruker AM 300 spectrometer equipped with a cross-polarization (CP) magic-angle spinning (MAS) accessory. Samples were packed in zirconia rotors (7 mm, <sup>29</sup>Si; 4 mm, <sup>11</sup>B, <sup>27</sup>Al) and spun in air. The <sup>29</sup>Si (59.63 MHz) NMR spectra were obtained at a spinning speed of 4 kHz, with recycle delays of 10 s for Bloch decay (BD) experiments and 2–5 s for CP experiments. Contact times for CP experiments were varied from 2.5 to 4.5 ms. The <sup>27</sup>Al (78.2 MHz) and <sup>11</sup>B spectra (96.3 MHz) were obtained at a spinning speed of 12 kHz (using fully hydrated samples in the case of Al). Additional <sup>29</sup>Si (99.38 MHz) BD and CP NMR experiments were carried out on a Bruker DSX500. In this case, a spinning speed of 8 kHz was used with 4 mm rotors. The DSX 500 was also used for <sup>71</sup>Ga (152.48 MHz) BD NMR experiments with a spinning speed of 12 kHz. In all cases, experiments were referenced externally (B, aq Boric acid = 18.8 ppm; Al, 1N Al(NO<sub>3</sub>)<sub>3</sub>; Si, tetrakisdimethylsilane; Ga, 1 N Ga(NO<sub>3</sub>)<sub>3</sub>). All reported <sup>29</sup>Si NMR results are from the 300 MHz instrument unless specifically noted. Field-emission scanning electron microscopy (FE-SEM) was performed using a Hitachi S-900 at the University of Tokyo. Prior to observation, the samples were dried in an oven at 85 °C, and coated by Pt for a few seconds using magnetron sputtering (Hitachi, E-1030). The acceleration voltage for the observation was varied between 7 and 10 kV. Nitrogen adsorption isotherms were obtained at 77 K using an Omnisorp 100 sorption apparatus operating in static mode using fixed dosing. Prior to the adsorption experiment, samples were treated under vacuum at 175 °C for at least 6 h. Vapor phase water adsorption isotherms were obtained on a McBain-Baker balance after pretreatment at 175–200 °C in situ. Nitrogen and water adsorption capacities are reported at *P/P*<sub>0</sub> = 0.05 and 0.2, respectively. Elemental analyses were performed at Galbraith Laboratories, Inc., Knoxville Tennessee.

## Results and Discussion

**Structural Characterization.** All of the samples used in this study are highly crystalline, as determined

(9) Skeels, G. W.; Breck, D. W. In *Proceedings of the 6th International Zeolite Conference*; Olson, D., Bisio, A., Eds.; Butterworths: Guilford, U.K., 1984; p 87.

(10) de Ruiter, R.; Pamin, K.; Kentgens, A. P. M.; Jansen, J. C.; van Bekkum, H. *Zeolites* **1993**, *13*, 611.

(11) Rigutto, M. S.; de Ruiter, R.; Niederer, J. P. M.; van Bekkum, H. *Stud. Surf. Sci. Catal.* **1994**, *84*, 2245.

(12) Takewaki, T.; Beck, L. W.; Davis, M. E. *J. Phys. Chem. B* **1999**, *103*, 2674.

(13) Takewaki, T.; Beck, L. W.; Davis, M. E. *Top. Catal.* **1999**, *9*, 35.

(14) Jones, C. W.; Tsuji, K.; Davis, M. E. *Microporous Mesoporous Mater.* **1999**, *33*, 223.

(15) Millini, R.; Perego, G.; Parker, W. O.; Bellussi, G.; Carluccio, L. *Microporous Mater.* **1995**, *4*, 221.

(16) Dwyer, J.; Zhao, J. *J. Mater. Chem.* **1992**, *2*, 235.

(17) Cambor, M. A.; Corma, A.; Valencia, S. *Chem. Commun.* **1996**, 2365.

(18) Tsuji, K.; Davis, M. E. *Microporous Mater.* **1997**, *11*, 53.

(19) Zones, S. I.; Yuen, L. T.; Toto, S. D. U.S. Patent 5,187,132, 1993.

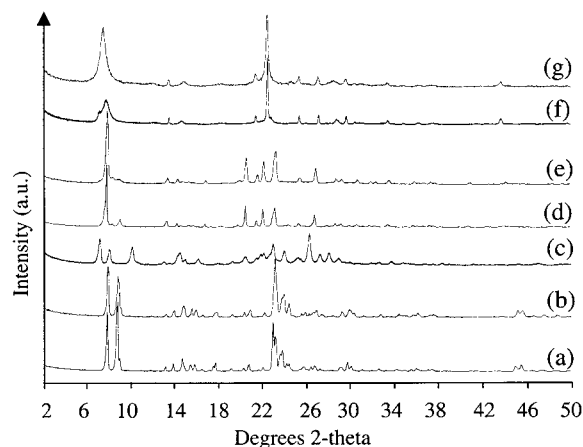


**Figure 1.** XRD patterns of calcined Si-MFI (a), B-MFI (b), ERB-1 (c), CIT-1 (d), SSZ-33 (e), B-Beta-F (f), and Si-Beta-OH (g).

by XRD and nitrogen physisorption analysis. The XRD patterns of several of the calcined samples are shown in Figure 1, and nitrogen capacities are given in Table 1. In most cases, the acetic acid treatment results in no notable changes in the XRD patterns of the samples (XRD patterns of CIT-1 and SSZ-33 after the acid treatment are shown in Supporting Information). Exceptions are the XRD patterns of ERB-1 which show an additional peak at  $2\theta = 3.5$  in samples extracted under all conditions, (see Supporting Information). This extra intensity is also seen in other all-silica materials with the MWW topology.<sup>20</sup>

In contrast to the XRD results, <sup>29</sup>Si BD NMR results show significant differences between the calcined and acetic acid treated molecular sieves in most cases. <sup>29</sup>Si BD NMR spectra for SSZ-33 treated with acetic acid for 6 days at a variety of temperatures are shown in Figure 2. As the temperature of the treatment is increased, the amount of Q<sup>3</sup> silicon in the sample decreases relative to Q<sup>4</sup> silicon. In addition, there is a significant sharpening of the Q<sup>4</sup> region, allowing crystallographically distinct T sites to be distinguished. These highly resolved NMR spectra can only result from expulsion of boron from the lattice and healing of the created framework defects with silicon. This loss of boron is confirmed by elemental analysis (Table 1). CIT-1, another borosilicate of the CON topology, behaves similarly. However, in this case, the most highly resolved NMR spectra (shown in Figure 3) appear slightly different from those of SSZ-33, likely due to the fact that SSZ-33 is an intergrowth of two polymorphs while CIT-1 is a single polymorph. High-silica samples of SSZ-33 and CIT-1 that are nearly free of defects have not been obtained previously. Reported attempts to produce materials of this nature by steaming were unsuccessful.<sup>3</sup>

The <sup>29</sup>Si BD NMR spectra of CIT-1 treated with acetic acid show at least five readily identifiable Q<sup>4</sup> silicon maxima at -109.35, -111.15, -111.95, -112.95, and -116.2 ppm. As there are seven crystallographically unique tetrahedral sites in the CON topology,<sup>3</sup> further deconvolutions of the spectra are required in order to identify all the sites. Figure 4 shows the experimental <sup>29</sup>Si BD NMR (500 MHz) spectrum of CIT-1 treated at

185 °C along with the simulated pattern. The pattern was successfully simulated using seven Lorentzian curves of nearly equal area, in agreement with the crystal structure of the CIT-1 (seven tetrahedral species of equal abundance). The experimental and simulated data are summarized in Table 2. Despite the fact that relatively short pulse delays are used (10 s), the simulated pattern agrees reasonably well with the published crystal structure.<sup>3</sup> For experiments using the 300 MHz instrument, a delay time of 10 s is used, whereas the delay is varied in experiments at 500 MHz. For delay times ranging from 10 to 60 s at 500 MHz, the overall relative intensity ratio remains almost constant while the signal continuously grows as the delay time is increased. An exception to this trend is the peak at -116.49 ppm, which requires a very long delay time (~100 s). This peak is therefore underestimated under the conditions used here. Nonetheless, the agreement between the NMR results and the published crystal structure with regard to T-site abundance is quite satisfactory under the conditions used here. More detailed structural characterization of these CIT-1 samples will be presented elsewhere.<sup>21</sup>

The <sup>29</sup>Si BD NMR spectra of acetic acid treated ERB-1 (MWW topology) are also markedly affected by the treatment conditions. Like the molecular sieves of the CON topology, treatment at higher temperatures yields materials with NMR spectra exhibiting fewer structural defects (Q<sup>3</sup> silicon) and increased T-site resolution in the Q<sup>4</sup> region. The NMR spectra are illustrated in Figure 5. The spectra of the acetic acid treated materials agree quite well with the published spectrum of ITQ-1, a silicate of the same MWW topology.<sup>22</sup> This result indicates that the present method is effective on materials that contain only 10 MR pore openings (MWW has also 12 MR pores that do not open to the exterior of the crystal) in addition to the CON materials that have 10 and 12 MR pore openings. Furthermore, the fact that the technique works on a material with a relatively high boron content (see Table 1) illustrates its versatility. While the <sup>29</sup>Si BD NMR spectra of the acetic acid treated materials exhibit essentially no Q<sup>3</sup> silicon, the materials are not perfectly defect-free, as evidenced by the <sup>29</sup>Si CP NMR spectra shown in Figure 6. Expulsion of boron from the lattice and healing of defects with silicon have an effect on the sorptive properties of the molecular sieves. In most cases, a minor loss in the nitrogen adsorption capacity is observed for the acetic acid treated samples, as shown in the data listed in Table 1. The silicon that heals the defect sites in the deboronated samples must originate from some portion of the sample, as no extra silicon source is included in the procedure. This slight loss in porosity is likely due to some dissolution of the crystal. FE-SEM results do not show many significant changes in crystal morphology after treatment with acetic acid (FE-SEM images of calcined SSZ-33, CIT-1, and ERB-1 are available in Supporting Information). For the cases of SSZ-33 and ERB-1, many different crystal habits are evident, with sizes ranging from tens of nanometers to several mi-

(21) Hwang, S. J.; Wilkinson, A. P.; Jones, C. W. manuscript in preparation.

(22) Cambor, M. A.; Corell, C.; Corma, A.; Diaz-Cabanas, M. J.; Nicolopoulos, S.; Gonzalez-Calbet, J. M.; Vallet-Regi, M. *Chem. Mater.* **1996**, *8*, 2415.

(20) Cambor, M. A.; Corma, A.; Diaz-Cabanas, M. J.; Baerlocher, C. *J. Phys. Chem. B* **1998**, *102*, 44.



**Table 1. Synthetic and Physical Parameters of Samples**

sample	topology <sup>a</sup>	treatment	pH <sup>b</sup>	temp. (°C)	time	Si/B <sup>c</sup>	N <sub>2</sub> ads (mL/g) <sup>d</sup>	H <sub>2</sub> O ads. (mL/g) <sup>e</sup>
CIT-1	CON	none				20.9	0.225	0.034
CIT-1	CON	aq acetic acid	1.65	160	6 days	>2000	0.244	0.013
CIT-1	CON	aq acetic acid	1.65	185	6 days	ND <sup>f</sup>	0.209	0.006
SSZ-33	CON	none				19.4	0.181	0.063
SSZ-33	CON	aq HCl	2.00	25	5 hours	ND	0.173	0.055
SSZ-33	CON	aq acetic acid	1.65	110	6 days	156.5	0.186	0.020
SSZ-33	CON	aq acetic acid	1.65	135	6 days	ND	0.186	0.017
SSZ-33	CON	aq acetic acid	1.65	160	6 days	ND	0.184	0.015
SSZ-33	CON	aq acetic acid	1.65	185	6 days	494.0	0.175	0.006
SSZ-33	CON	aq acetic acid	1.65	135	14 days	ND	0.173	0.009
ERB-1	MWW	none				10.9	0.165	0.045
ERB-1	MWW	aq HCl	2.00	25	5 hours	36.5	0.159	0.087
ERB-1	MWW	aq acetic acid	1.65	135	6 days	75.0	0.170	0.036
ERB-1	MWW	aq acetic acid	1.65	160	6 days	ND	0.164	0.013
ERB-1	MWW	aq acetic acid	1.65	185	6 days	ND	0.146	0.007
ERB-1	MWW	aq acetic acid	1.65	185	6 days	ND	0.141	0.011
Si-MFI	MFI	none					0.144	0.011
Si-MFI	MFI	aq acetic acid	1.65	185	6 days		0.153	0.013
B-MFI	MFI	none				51.4	0.138	0.019
B-MFI	MFI	aq acetic acid	1.65	135	6 days	>900	0.143	0.013
B-MFI	MFI	aq acetic acid	1.65	185	6 days	>400	0.140	0.009
Si-Beta-OH	*BEA	none					0.285	0.045
Si-Beta-OH	*BEA	aq acetic acid	1.65	135	6 days		0.248	0.047
Si-Beta-OH	*BEA	aq acetic acid	1.65	160	6 days		0.226	0.030
B-Beta-F	*BEA	none				29.2	0.231	0.039
B-Beta-F	*BEA	aq acetic acid	1.65	135	6 days	>350	0.239	0.039
B-Beta-F	*BEA	aq acetic acid	1.65	185	6 days	>1000	0.099 <sup>g</sup>	0.011

<sup>a</sup> International Zeolite Association structure code. <sup>b</sup> Initial solution pH. <sup>c</sup> Si/B ratio as determined by elemental analysis. <sup>d</sup> As determined by nitrogen adsorption, 77 °C  $P/P_0 = 0.05$ . <sup>e</sup> Water adsorption on a McBain–Baker balance, 25 °C,  $P/P_0 = 0.2$ . <sup>f</sup> ND = not determined. <sup>g</sup> Some structural collapse.

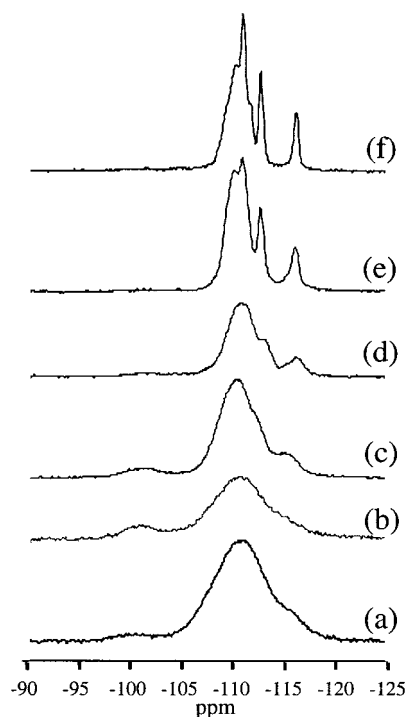


**Figure 2.** <sup>29</sup>Si BD NMR spectra of calcined SSZ-33 (a), calcined SSZ-33 that was deboronated by treatment with 0.01 N HCl for several hours (b) and calcined SSZ-33 treated with acetic acid for 6 days at 110 (c), 135 (d), 160 (e), and 185 °C (f).

crons. After treatment at various temperatures with aqueous acetic acid, the FE–SEM images of the materials are virtually unchanged with regard to particle morphology. However, when the materials are treated in a manner that results in solids where nearly all of their defects are healed as judged by <sup>29</sup>Si BD NMR, notable changes in surface features are apparent in

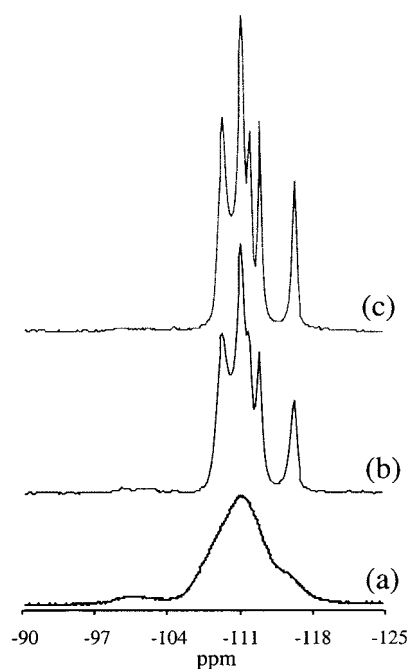


**Figure 3.** <sup>29</sup>Si BD NMR spectra of calcined CIT-1 (a) and CIT-1 treated with acetic acid for 6 days at 160 (b) and 185 °C (c).

some of the FE–SEM images. Figure 7 shows the FE–SEM images of SSZ-33 treated at 110 °C for 6 days (defects not healed), SSZ-33 treated at 135 °C for 14 days and 185 °C for 6 days (defects healed), and calcined SSZ-33 for comparison. For the SSZ-33 samples where the defects have been healed, triangular mesopores are evident in the samples. The number of mesopores appears to be higher on samples treated at the higher temperature. In Figure 7d (185 °C treatment), very small particles are visible on the surface of the crystals

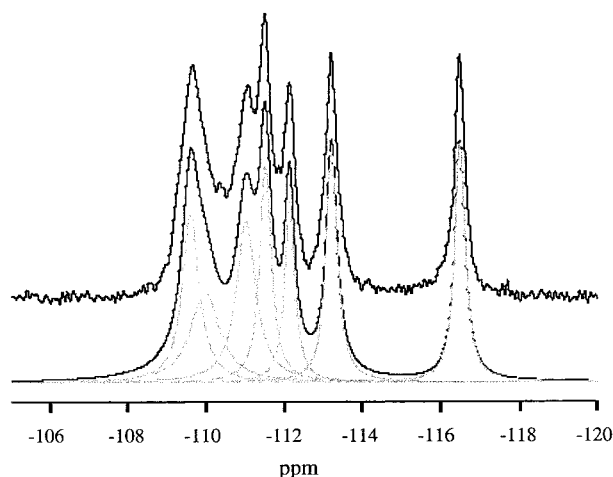


**Figure 4.** Simulated (bottom) and experimental (top) 500 MHz  $^{29}\text{Si}$  BD NMR spectra of CIT-1 treated at 185 °C.

**Table 2. Assignment of  $^{29}\text{Si}$  BD NMR Lines of CIT-1 Extracted at 185 °C**

300, <sup>a</sup> d <sup>b</sup>	500, <sup>c</sup> d <sup>b</sup>	300, <sup>a</sup> I <sup>d</sup>	500, <sup>c</sup> I <sup>d</sup>	300, <sup>a</sup> fwhm <sup>e</sup>	500 <sup>c</sup>
-109.49	-109.61	1.1	1.1	0.635	0.515
-109.93	-109.98	1.1	1.0	0.948	0.870
-111.16	-111.03	1.3	1.2	0.736	0.600
-111.5	-111.53	1.3	1.0	0.441	0.358
-112.2	-112.15	0.9	0.7	0.489	0.302
-113.2	-113.22	0.9	1.0	0.389	0.338
-116.45	-116.49	0.8	0.9	0.482	0.311

<sup>a</sup> In megahertz with a 10 s pulse delay. <sup>b</sup> Chemical shift, in parts per million. <sup>c</sup> In megahertz with a 60 s pulse delay. <sup>d</sup> Intensity, (normalized; crystal structure predicts all should have intensity = 1). <sup>e</sup> Full width at half-maximum.

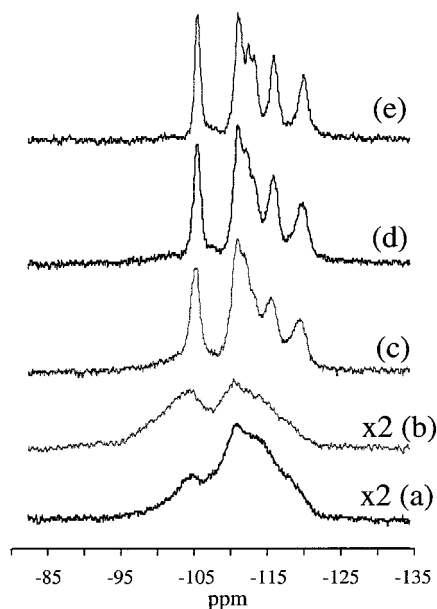


**Figure 5.**  $^{29}\text{Si}$  BD NMR spectra of calcined ERB-1 (a), calcined ERB-1 that was deboronated by treatment with 0.01 N HCl for several hours (b) and calcined ERB-1 treated with acetic acid for 6 days at 135 (c), 160 (d), and 185 °C (e).

that are not present in the other images. These particles may result from dissolution of the small spherical particles in the sample. Another possibility is that they originate from silica that was previously part of the large crystals in the locations of the mesopores.

The presence of the mesopores is important for two reasons. First, it indicates that the silica required to

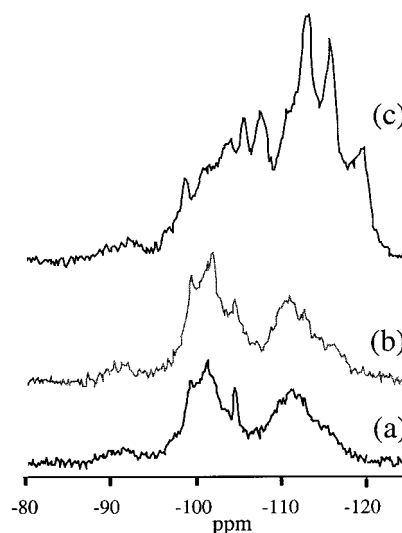


**Figure 6.**  $^{29}\text{Si}$  CPMAS NMR spectra of CIT-1 (a), SSZ-33 (b), and ERB-1 (c) with a 2.5 ms contact time.

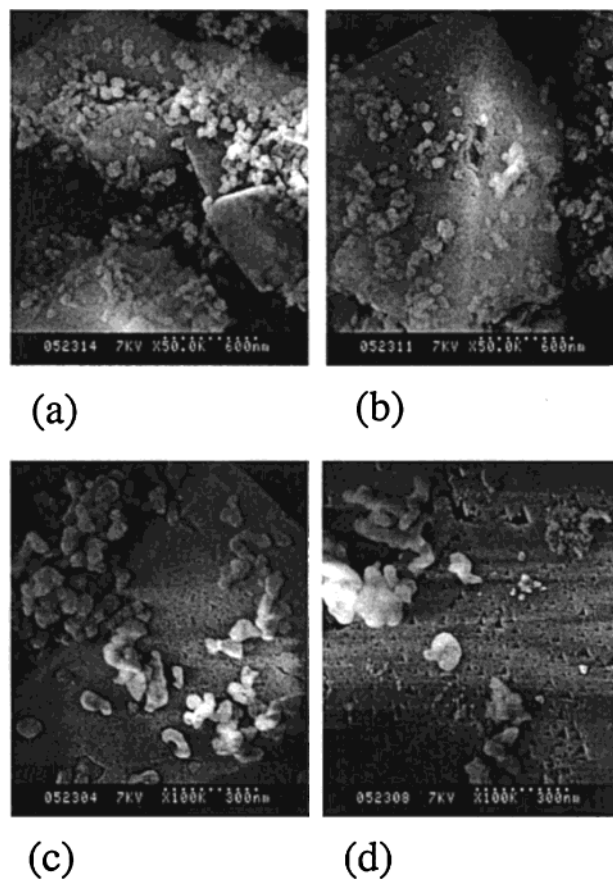


**Figure 7.** FE-SEM images of calcined SSZ-33 (a) and calcined SSZ-33 treated at 110 °C for 6 days (b), treated at 135 °C for 14 days (c) and treated at 185 for 6 days (d).

heal the defect sites of the materials may come from the crystal itself, rather than from the smaller particles present via an Ostwald's ripening mechanism. This observation, however, does not rule out the possibility that the smaller crystals are dissolved in order to provide silica that heals defects in the larger ones, although the relative abundances of the small and large particles do not appear to change after treatment with acetic acid. The second important implication of the presence of mesopores concerns the transport of soluble

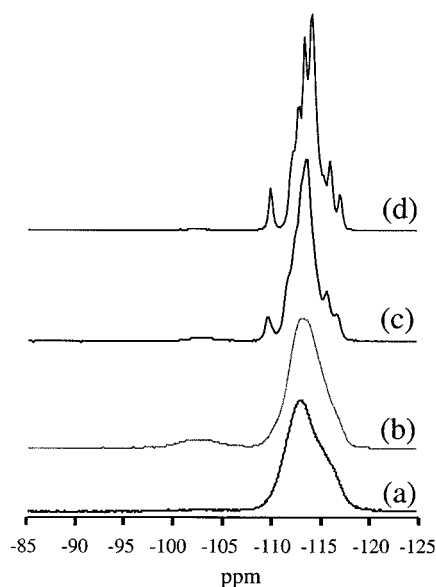


**Figure 8.**  $^{29}\text{Si}$  BD NMR spectra of calcined B-MFI (a), calcined B-MFI treated with acetic acid at 185 °C for 6 h (b), calcined Si-MFI (c), and calcined Si-MFI treated with acetic acid at 185 °C for 6 h (d).

silica species, as the presence of large mesopores would greatly enhance the movement of these species through the pores to the defect sites that they must heal. Note that although mesopores are detected clearly by FE-SEM, significant differences in the nitrogen physisorption isotherms of materials with and without mesopores were not detected due to the low cutoff pressure of the experiments (200 Torr).

Another consequence of the expulsion of boron and healing the defects with silicon is an increase in hydrophobicity. The data in Table 1 illustrate that there is a significant decline in the water adsorption capacities of the materials after treatment with acetic acid, indicating increased hydrophobicity resulting from replacement of boron with silicon in the lattice. The hydrophobicity as measured by the water adsorption uptake correlates nicely with the population of  $\text{Q}^3$  silicon as determined by  $^{29}\text{Si}$  BD NMR (less  $\text{Q}^3$  silicon = lower water adsorption). Furthermore, the hydrophobicities of the materials compare well with those of calcined, defect-free materials such as calcined, pure-silica Beta synthesized in fluoride media ( $<0.01 \text{ cm}^3/\text{g}^{14}$ ).

On some materials, the effect of the acid treatment is not as pronounced as that illustrated above. For example, when calcined B-MFI is treated with aqueous acetic acid, boron is expelled from the framework but only a fraction of the defects are healed (from the  $^{29}\text{Si}$  BD NMR spectra shown in Figure 8). Further evidence of the transformation from the borosilicate to the pure-silicate is the increased hydrophobicity of the treated material (Table 1) and the development of additional uptake in the nitrogen physisorption experiment due to nitrogen restructuring (see Supporting Information). This restructuring is well-known in pure-silica MFI materials but uncommon in heteroatom-containing MFI samples.<sup>23</sup> Of note is the fact that the value of  $PP_0$  at which the nitrogen restructuring occurs in the isotherm

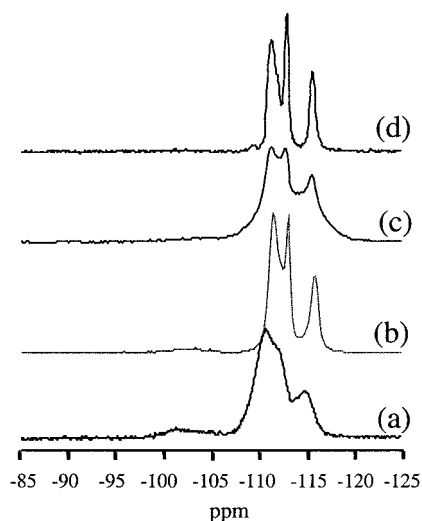


**Figure 9.**  $^{29}\text{Si}$  BD NMR spectra of calcined B-Beta-F (a), calcined B-Beta-F treated at 135 °C for 6 days (b), calcined B-Beta-F treated at 185 °C for 6 days (c), and calcined, defect-free all-silica Beta synthesized in fluoride media (d).

of the acetic acid treated B-MFI ( $P/P_0 = 0.05\text{--}0.07$ ) differs from that of Si-MFI ( $P/P_0 = 0.15\text{--}0.18$ ). This may be due to differences in crystal morphology or the number of internal defects (polar adsorption sites can affect the dipolar interactions in nitrogen)<sup>23b</sup> in each sample.

All-silica MFI (Si-MFI) was also treated with acetic acid solution in an effort to heal anionic defects originating from the charge-balancing TPA in the hydroxide mediated synthesis.<sup>24</sup> In this case, the  $^{29}\text{Si}$  BD NMR spectrum (Figure 8) sharpens to appear more like a defect-free, all-silica material synthesized in fluoride media, although some visible  $\text{Q}^3$  silicon species at  $-102.5 \text{ ppm}$  clearly remain. The apparent lower efficiency of the treatment on molecular sieves with the MFI topology may be due to the small pore apertures that could limit migration of soluble silica species.

A series of molecular sieves with the \*BEA structure were also subjected to the acetic acid treatment. Si-Beta-OH, a nanocrystalline all-silica Beta material, did not show significant increases in hydrophobicity (Table 1) after treatment with acetic acid solutions nor did it exhibit significantly less  $\text{Q}^3$  silicon in the  $^{29}\text{Si}$  BD NMR experiments, although significant changes in nitrogen sorption capacities (Table 1) indicated significant solid dissolution had taken place. Similarly, a nanocrystalline B-Beta sample synthesized in hydroxide media also showed significant levels of  $\text{Q}^3$  silicon in  $^{29}\text{Si}$  BD NMR experiments. In contrast to the results obtained with the nanocrystalline samples, a boron Beta sample with significantly larger crystals, B-Beta-F, could successfully be deboronated with healing of the subsequent defect sites during aqueous acetic acid treatment. However, this material was very sensitive to the temperature of the treatment. As demonstrated by the nitrogen adsorption data in Table 1, extraction at lower temperatures was useful for deboronating the molecular sieve and maintaining good crystallinity, whereas higher temperatures led to a significant loss of porosity. Figure 9

(23) (a) Carrott, P. J. M.; Sing, K. S. W. *Chem. Ind.* **1986**, 786. (b) Sing, K. S. W.; Carrott, P. J. M. *Chem. Ind.* **1993**, 165.

(24) Flanigan, E. M.; Bennett, J. M.; Grose, R. W.; Cohen, J. P.; Patton, R. L.; Kirchner, R. M.; Smith, J. V. *Nature* **1978**, 271, 512.

Table 3. Synthetic and Physical Parameters of Samples Used in Control Experiments

sample	topology <sup>a</sup>	treatment	pH <sup>b</sup>	temp. (°C)	time	Si/B <sup>c</sup>	N <sub>2</sub> ads (mL/g) <sup>d</sup>	H <sub>2</sub> O ads. (mL/g) <sup>e</sup>
Variation of Acid								
SSZ-33	CON	aq acetic acid	1.65	135	6 days	ND <sup>f</sup>	0.186	0.017
SSZ-33	CON	aq HCl	1.30	135	6 days	ND	0.178	0.016
SSZ-33	CON	aq HNO <sub>3</sub>	1.30	135	6 days	ND	0.168	0.014
SSZ-33	CON	aq H <sub>2</sub> SO <sub>4</sub>	1.30	135	7 days	ND	0.170	0.020
Variation of pH and Temperature								
SSZ-33	CON	aq acetic acid	0.75	135	6 days	196.0	0.186	0.028
SSZ-33	CON	aq acetic acid	1.65	135	6 days	ND	0.186	0.017
SSZ-33	CON	aq acetic acid	2.50	135	6 days	66.9	0.154	0.027
SSZ-33	CON	aq acetic acid	0.90	185	6 days	ND	0.193	0.004
SSZ-33	CON	aq acetic acid	1.65	185	6 days	494.0	0.175	0.006
SSZ-33	CON	aq acetic acid	2.50	185	6 days	ND	0.076	ND
Additional Iterations								
SSZ-33	CON	water, Al(NO <sub>3</sub> ) <sub>3</sub>	ND	95	3 days	56.7 <sup>g,h</sup> (199)	0.186	0.065
SSZ-33	CON	aq acetic acid, Al(NO <sub>3</sub> ) <sub>3</sub>	1.65	160	6 days	56.3 <sup>h</sup>	0.175	0.059
SSZ-33	CON	water, Ga(NO <sub>3</sub> ) <sub>3</sub>	ND	95	3 days	45.1 <sup>i</sup>	0.189	ND
SSZ-33	CON	aq acetic acid, Ga(NO <sub>3</sub> ) <sub>3</sub>	1.65	160	6 days	78.1 <sup>i</sup>	0.175	ND
SSZ-33	CON	aq acetic acid <sup>j</sup>	1.65	135	6 days	ND	0.167	0.009
SSZ-33	CON	aq acetic acid <sup>k</sup>	1.65	135	6 days	ND	amor. <sup>l</sup>	ND
ERB-1	MWW	aq acetic acid <sup>j</sup>	1.65	185	6 days	ND	0.141	0.011

<sup>a</sup> International Zeolite Association structure code. <sup>b</sup> Initial solution pH. <sup>c</sup> Si/B ratio as determined by elemental analysis. <sup>d</sup> As determined by nitrogen adsorption,  $P/P_0 = 0.05$ . <sup>e</sup> Water adsorption on a McBain–Baker balance, 25 °C,  $P/P_0 = 0.2$ . <sup>f</sup> ND = not determined. <sup>g</sup> Si/B ratio in parentheses after treatment. <sup>h</sup> Si/Al ratio as determined by elemental analysis. <sup>i</sup> Si/Ga ratio as determined by elemental analysis. <sup>j</sup> Solution presaturated with soluble SiO<sub>2</sub> species. <sup>k</sup> Solution presaturated with soluble GeO<sub>2</sub> species. <sup>l</sup> Structural collapse leaving nonporous, amorphous material.

shows <sup>29</sup>Si BD NMR spectra for B–Beta–F treated under different conditions along with the spectrum of calcined, defect-free all-silica Beta synthesized in fluoride media for comparison. Particularly noteworthy is the change in the spectrum after treatment at 185 °C (Figure 9c), conditions that lead to significant structural collapse. This loss in crystallinity can also be seen visually upon inspection of the FE–SEM image of the 185 °C treated material (images of \*BEA materials are provided in Supporting Information). This observed loss in porosity at higher treatment temperatures has been documented previously during the extraction of the tetraethylammonium fluoride structure-directing agent from as-synthesized \*BEA materials using aqueous acetic acid solutions<sup>14,25</sup>

**Control Studies.** Numerous experiments were carried out on the SSZ-33 material to ascertain information concerning the role of acetic acid and the mechanism of defect repopulation. Samples were treated under a variety of conditions, with temperature, pH, and the type of solution used as the major variables. Descriptions of the various experiments and the characterization of the resulting samples are tabulated in Table 3. Varying the nature of the acid over a narrow range of pH (1.3–1.75) had little effect on the properties of the resulting material. Use of an organic acid such as acetic acid or different mineral acids that included nitric, sulfuric, and hydrochloric all successfully deboronated SSZ-33 and healed the resulting defects to a similar degree (ascertained by the amount of Q<sup>3</sup> silicon that is apparent in the <sup>29</sup>Si BD NMR spectra). The mineral acids appear to give materials with slightly sharper Q<sup>4</sup> regions in the <sup>29</sup>Si BD NMR spectra. In addition, treatment with mineral acids results in materials with more significant porosity losses than those from treatment with acetic acid. This may indicate that the mineral acids more readily solubilize silica than does the

organic acid. Similar results have been observed while extracting TEAF from all-silica Beta using both aqueous hydrochloric acid and acetic acid at the same pH (pH = 1.65, 80 °C, 12 h, 2×). Both treatments completely remove TEAF from the pores of the molecular sieve but the mineral acid treatment results in significant formation of mesopores as determined by nitrogen physisorption measurements.<sup>26</sup>

Variations in the pH appear to have a significant affect on the resulting properties of the solids. Figure 10 contains the <sup>29</sup>Si BD NMR spectra of the SSZ-33 material treated at various pHs and at two temperatures, 135 and 185 °C. pH adjustment was carried out by increasing the amount of acetic acid relative to water to achieve more acidic conditions or by adding aqueous sodium hydroxide to the standard mixture of acetic acid and water to achieve more basic conditions. At 135 °C, the amount of Q<sup>3</sup> silicon decreases, and the sharpness of the Q<sup>4</sup> region increases upon moving from a pH of 2.5 to 1.65. However, at a pH of 0.75, the results are generally poorer. This is may be due to the high organic content of the treatment solution (60% acetic acid) that may limit the solubility of dissolved silica species. For treatment at 185 °C, the low and moderate pHs gave hydrophobic materials with well-resolved <sup>29</sup>Si BD NMR spectra. However, at a pH of 2.5, structural degradation occurred, and both the XRD powder pattern and nitrogen adsorption results were indicative of a partially amorphous material. Apparently, the presence of the added sodium used to adjust the pH of the solution leads to loss of crystallinity at high temperatures. A similar result was obtained upon treatment at a pH of 3.5.

**Mechanism of Deboronation and Defect Repopulation.** The effect of acidic solutions on microporous metallosilicates, especially aluminosilicates<sup>6,27</sup> and borosilicates<sup>10</sup> is well-documented. Aqueous acids

(25) Jones, C. W.; Tsuji, K.; Takewaki, T.; Beck, L. W.; Davis, M. E. *Microporous Mesoporous Mater.* in press.

(26) Jones, C. W.; Davis, M. E. unpublished results, 2000.

(27) Lee, E. F. T.; Rees, L. V. C. *J. Chem. Soc., Faraday Trans. 1* **1987**, 83, 1531.



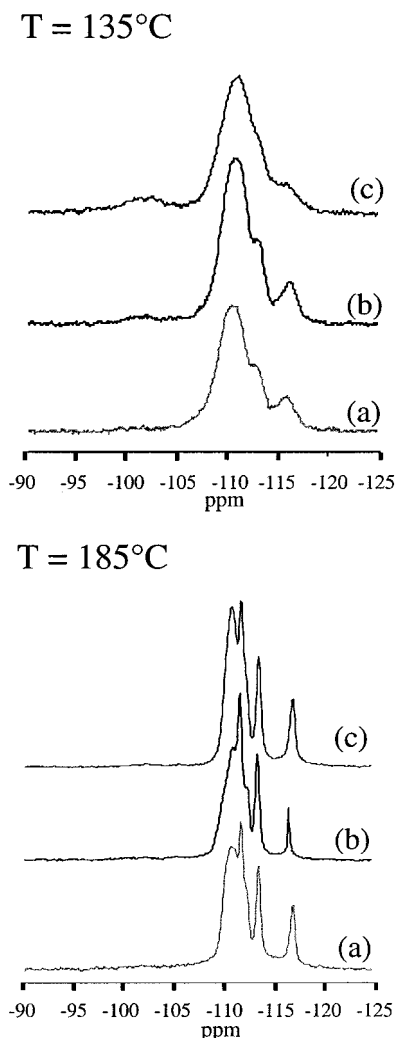


**Figure 10.**  $^{29}\text{Si}$  BD NMR spectra of calcined SSZ-33 treated for 6 days at various pHs and temperatures. At 135 °C: pH 2.5 (a), 1.65 (b), and 0.75 (c). At 185 °C: pH 2.5 (a), 1.65 (b), and 0.90 (c).

are efficient hydrolyzing agents for the removal of boron and aluminum from the framework, leaving behind silanol nests with Si—O(H) groups that are positioned for the incorporation of other tetrahedral species such as titanium or silicon. Rees and co-workers showed the importance of pH during dealumination of zeolite NaY with hydrochloric acid; dealumination did not occur above a pH of 2.3, and complete dealumination occurred below a pH of 0.46.<sup>27</sup> Researchers at Mobil characterized in detail zeolite Beta samples that were dealuminated by aqueous oxalic acid treatments.<sup>28</sup> They showed using FTIR spectroscopy that samples dealuminated for extended periods of time with the diacid solution (pH 0.5–1.0) contained a reduced number of silanol species attributed to either adjacent silanol condensation or silica migration, an observation in agreement with results presented here. However, complete removal of aluminum was not obtained, and only a fraction of the silanol defects were healed. In contrast, Prins and co-workers report that significant structural defects remained after dealumination of mordenite with oxalic acid.<sup>29</sup> van Bekkum and co-workers have reported that

high-silica molecular sieves can be synthesized from borosilicates by the deboronation of the materials at room temperature with aqueous hydrochloric acid followed by subsequent insertion of silicon species into the vacancies by treatment with tetramethyl orthosilicate or dichloromethylsilane in the liquid phase.<sup>10</sup> This two-step procedure could give partial silylation of the silanol nests to make a high-silica material with relatively few defects (although high levels of repopulation were not achieved). Single-step treatments of the calcined borosilicate with  $\text{SiCl}_4$  were reported to give a substantial loss in crystallinity.<sup>10</sup> In contrast, by use of the method reported here, nearly complete removal of boron with simultaneous healing of silanol nests by silicon could be achieved in a single step without the addition of any extra silica sources. Additionally, minor porosity losses are incurred with this method.

Further investigations were carried out to probe the possibility of filling the defect sites with species other than silicon. A fraction of the defects were healed by aluminum or gallium using the following procedure:<sup>30</sup> calcined SSZ-33 was added to an aqueous solution of aluminum nitrate or gallium nitrate in a plastic bottle and heated in an oven for 3 days at 95 °C. Subsequently, the solid was recovered by filtration and washed with 0.01 N HCl and water. By use of this technique, a portion of the defect sites are filled with the trivalent cation, and the remaining sites are left vacant, to give a metallosilicate with internal defects when the amount of added Al or Ga is less than the total number of silanol nests resulting from deboronation. For comparison, calcined SSZ-33 was also treated with an equal amount of aluminum or gallium in aqueous acetic acid and heated at 160 °C for 6 days following the acetic acid treatment procedure outlined here. Figure 11 shows the  $^{29}\text{Si}$  BD NMR spectra of deboronated SSZ-33 and SSZ-33 treated with aluminum using the organic-free procedure<sup>30</sup> and the acetic acid procedure. After population of a portion of the defect sites with the aluminum using the organic-free procedure, the  $^{29}\text{Si}$  BD NMR spectrum clearly shows the presence of both incorporated aluminum and remaining silanols. The  $^{29}\text{Si}$  CPMAS NMR spectrum shows a strong  $\text{Q}^3$  silicon signal near -102 ppm and that the signal at -104 ppm in the BD spectrum is attributable to  $\text{Si}(\text{OSi})_3\text{OAl}$ . The material contacted with acetic acid containing dissolved aluminum cations retains far fewer defect silanols than the material treated with the other insertion procedure. These results indicate that a large portion of the defect silanols can be healed while simultaneously inserting aluminum into a portion of the vacancies. Water adsorption data in Table 3 indicate that insertion in the presence of acetic acid results in a more hydrophobic aluminosilicate. As expected, the materials treated with acetic acid suffered from a minor loss in nitrogen capacity.<sup>27</sup>  $^{27}\text{Al}$  BD NMR results indicate that the aluminum in the samples is mostly tetrahedrally coordinated (tetrahedral peak at 57.9 ppm, octahedral peak at 0.4 ppm, spectra not shown). The acetic acid treated material was found to contain less extraframework aluminum (~2%) than the material prepared using the

(28) Apelian, M. R.; Fung, A. S.; Kennedy, G. J.; Degnan, T. F. *J. Phys. Chem.* **1996**, *100*, 16577.

(29) Giudici, R.; Kouwenhoven, H. W.; Prins, R. *Appl. Catal. A* **2000**, *203*, 101.

(30) Jones, C. W.; Zones, S. I.; Davis, M. E. *Microporous Mesoporous Materials* **1999**, *28*, 471 and references therein.

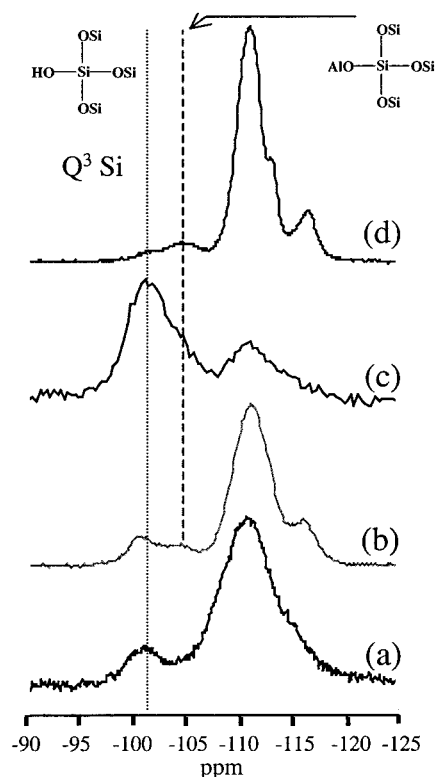


**Figure 11.**  $^{29}\text{Si}$  NMR spectra of calcined, deboronated SSZ-33 (a), calcined SSZ-33 treated with aqueous  $\text{Al}(\text{NO}_3)_3 \cdot 9\text{H}_2\text{O}$  and  $^{29}\text{Si}$  BD NMR (b), calcined SSZ-33 treated with aqueous  $\text{Al}(\text{NO}_3)_3 \cdot 9\text{H}_2\text{O}$  and  $^{29}\text{Si}$  CP NMR (c), and calcined SSZ-33 treated with  $\text{Al}(\text{NO}_3)_3 \cdot 9\text{H}_2\text{O}$ -containing acetic acid solution at 160 °C for 6 days and  $^{29}\text{Si}$  BD NMR (d).

other procedure (~10%). Similar results were obtained with the gallium treated materials.  $^{71}\text{Ga}$  BD NMR spectra of both gallium-inserted samples have only a single resonance assigned to tetrahedral gallium at 166 ppm.

Apparently, silicon species must migrate from one portion of the crystal to another in order to heal the defect sites during the acid treatment. This migration has been considered to occur by two potential mechanisms in other systems. The first mechanism can be described as a T-jump<sup>31</sup> mechanism whereby defect sites *apparently* migrate from the internal portions of the crystal to the surface of a crystal (without the dissolution of a discrete, solublized, monomeric species) in the presence of steam at high temperatures. This process is thought to occur in the ultrastabilization process of zeolite Y. The second mechanism involves the dissolution of one part of the crystal followed by diffusion of monomeric or oligomeric silica species through the micropores followed by subsequent incorporation into the defect sites.

The presence of mesopores detectable by FE-SEM in materials that were nearly free of  $\text{Q}^3$  silicon defect sites illustrates a possible source for dissolved silica species as well as pathways for rapid transport of the dissolved silica species, as mentioned above. This observation implies that mechanism two described above may operate under the conditions described here. To further probe this possibility, experiments were carried out

using an acetic acid solution presaturated with dissolved silica species. An acetic acid solution was heated in an autoclave with Cab-O-Sil M5 silica for several days at 135–185 °C, then separated from the remaining fumed silica while still warm, and subsequently added to autoclaves filled with SSZ-33 and ERB-1. These autoclaves were then treated at 185 °C for 6 days in the standard manner, and the resulting molecular sieves were recovered and characterized. The data listed in Table 3 indicate that using this treatment method results in materials that are not significantly different from when the silica presaturation step is omitted. It was hypothesized that presaturating the solution with soluble silica species would prevent significant degradation of the crystals via silica dissolution, giving increased micropore volume. However, the procedure used here resulted in materials with slightly lower microporosities and modestly higher water affinities. This result could possibly be attributed to the deposition of dissolved silica from the solution onto the crystals. This deposition might occur if the presence of mesopores is needed for efficient transport of the dissolved silica species, as no mesopores would be present at the outset of the experiment. Similar experiments with dissolved germanium oxide and SSZ-33 resulted in complete loss of crystallinity and porosity as determined by XRD and nitrogen physisorption (Table 3).

These results indicate that dissolved silica species that are in the bulk solution outside the crystals may not be useful for healing the internal defects of the solids. This observation would support the idea that only locally dissolved silica species at each crystallite are capable of migrating through the crystal and healing the defect sites and would argue for a mechanism that does not include an Ostwald's ripening behavior. The fact that the procedure also works for CIT-1 and B-Beta-F, materials composed almost entirely of large crystals, argues against the importance of an Ostwald's ripening mechanism as well. From these results, it appears that an Ostwald-like process is not important under the conditions used, although the contribution of such a mechanism cannot explicitly be ruled out in cases where both very small and very large particles exist in a sample.

**Role of Solution pH and Temperature.** The results here indicate that the treatment is most effective at removing boron and healing the defects with silicon when the solution pH is slightly below the isoelectric point of silica (pH ~ 2). Iler divides the behavior of aqueous silicates into three regions of pH: pH > 7, 2 < pH < 7, and pH < 2.<sup>32–33</sup> At pH's in excess of 7, condensation occurs by nucleophilic attack of  $\text{OH}^-$ . In the pH range of 2–7, the same mechanism is thought to occur, with the condensation rate proportional to the concentration of  $\text{OH}^-$ . In contrast, below a pH of 2, the rate is proportional to the concentration of  $\text{H}^+$  (in the absence of  $\text{F}^-$ ). It is under these conditions, where the solubility of silica is low (0 < pH < 2), that acid treatment is shown here to be very effective at producing nearly defect-free, pure silicates from borosilicates or zincosilicates<sup>12</sup> without an external silicon source. At

(31) Kornatowski, J.; Baur, W. H.; Pieper, G.; Rozwadowski, M.; Schmitz, W.; Cichowlas, A. *J. Chem. Soc., Faraday Trans.* **1992**, *88*, 1339 and references therein.

(32) Brinker, C. J.; Scherer, G. W. *Sol-Gel Science*; Academic Press: New York, 1990; p 103.

(33) Iler, R. K. *The Chemistry of Silica*; Wiley: New York, 1979.

these conditions, the dissolution of the molecular sieve is slow enough to prevent significant loss of microstructure while at the same time allowing sufficient dissolution of silica to provide soluble species for healing of the defects.

The use of the aqueous acetic acid treatment on molecular sieves was first used to extract TEAF from the pores of OFMSs<sup>12,34</sup> and subsequently applied to CIT-6 for a similar purpose.<sup>12</sup> In both cases, it was found that extraction with TEAF produced completely porous materials that were nearly free of structural defects. In contrast, extraction of OFMSs with aqueous pyridine (pH > 7) or a 50/50 mixture of pyridine and 1 N HCl (pH = 5.65), as well as extraction of CIT-6 with 1 N  $\text{NH}_4\text{NO}_3$  (pH = 4.8)<sup>12–13,25</sup> gave porous materials that contained internal structural defects.<sup>12</sup> In light of the results presented here, it is clear that pH is an overriding factor that controls the presence or absence of structural defects during extraction of SDAs or in the treatment of calcined molecular sieves. By use of the treatment in acidic media ( $0 < \text{pH} < 2$ ), materials that are nearly free of defects can be prepared from Si-Beta or OFMSs made from TEAF,<sup>14,25</sup> Si-Beta made using TEAOH,<sup>35</sup> and CIT-6 (zincosilicate Beta) prepared with TEAOH.<sup>12,25</sup> Similarly, we show here that materials essentially free of defects can be synthesized from calcined SSZ-33, B-Beta, CIT-1, and ERB-1 using similar treatments.

An equally important factor to pH is temperature. Materials that are in essence free of defects can be prepared with no loss of porosity relative to the calcined materials during SDA extraction in aqueous acetic acid at temperatures below 100 °C when the molecular sieves contain  $\text{F}^-$  (OFMSs and Si-Beta made from TEAF). At elevated temperatures, some porosity is lost (likely due to structural degradation by  $\text{F}^-$ ). In contrast, CIT-6 (which is synthesized in  $\text{OH}^-$  media) treated with acetic acid under 100 °C leaves a porous all-silica material with many defects. Treatment at temperatures above 100 °C is required to heal the defects. Hence, in the absence of  $\text{F}^-$ , the healing of defects by silicon requires

higher temperatures. A similar trend is observed from treatment of calcined materials. In this case, moderate temperatures (135 °C) are required to expel boron from calcined B-Beta-F and heal defects, whereas higher temperatures lead to significant structural degradation, possibly due to traces of residual  $\text{F}^-$ . For materials that contain no  $\text{F}^-$ , such as ERB-1, SSZ-33, or CIT-1 (molecular sieves that were synthesized in hydroxide media), higher temperatures give better results (160–185 °C) with limited loss in porosity due to structural degradation. Hence, as observed during SDA extraction from as-made molecular sieves, calcined samples synthesized in the presence of  $\text{F}^-$  require lower temperatures for effective healing of defects with silicon.

## Conclusions

Hydrothermal treatment of calcined borosilicates and silicates with aqueous acetic acid near the isoelectric point of silica (pH = 0–2) effectively produces hydrophobic silicates with few structural defects. Defect sites are healed via dissolution of silica within the crystal, creating mesopores, followed by migration of the solubilized silica throughout the material to heal internal defects. Solution pH and temperature are found to be important variables in controlling the properties of the resulting materials, with higher temperatures resulting in samples with fewer defects but slightly less porosity. Mineral acids can be substituted for organic acids.

By use of this technique, all-silica CIT-1 and SSZ-33 are synthesized for the first time. CIT-1 with very few internal defects is characterized by  $^{29}\text{Si}$  MAS NMR spectroscopy and reveals seven unique silicon atoms, in agreement with the published crystal structure.

**Acknowledgment.** This work was partially supported by Chevron. C.W.J. thanks Akzo Nobel and BP Amoco for additional financial support.

**Supporting Information Available:** XRD patterns and FE-SEM images of CIT-1, SSZ-33, ERB-1, and so on;  $^{29}\text{Si}$  BD NMR spectra of Si-Beta-OH and B-Beta-OH; nitrogen physisorption isotherms for B-MFI and Si-MFI (PDF). This material is available free of charge via the Internet at <http://pubs.acs.org>.

CM0007961

(34) Jones, C. W.; Tsuji, K.; Davis, M. E. *Nature* **1998**, *393*, 52.

(35) Takewaki, T.; Hwang, S. J.; Yamashita, H.; Davis, M. E. *Microporous Mesoporous Mater.* **1999**, *32*, 265.